Supporting Information

Modulation of two-dimensional palladium nanozyme activity to enhance chemodynamic/photothermal combined therapy for melanoma

Duo Sun,[†a] Kaijun Liu,[†b] Yi Cheng,[†b] Jinju Sun,[a] Jingqin Fang,[c] Yi Tang, [a] Fangyang Wang,[a] Yu Guo,[d] Yi Wang,[*a] Xiao Chen,[* a,e]

[a]Department of Nuclear Medicine, Daping Hospital, Army Medical University, Chongqing, 400042, China.

[b]Department of Gastroenterology, Daping Hospital, Army Medical University, Chongqing, 400042, China.

[c]Department of Ultrasound, Daping Hospital, Army Medical University, Chongqing, 400042, China.

[d]Department of Radiology, Daping Hospital, Army Medical University, Chongqing, 400042, China.

[e]Chongqing Clinical Research Center for Imaging and Nuclear Medicine, Chongqing, 400042, China.

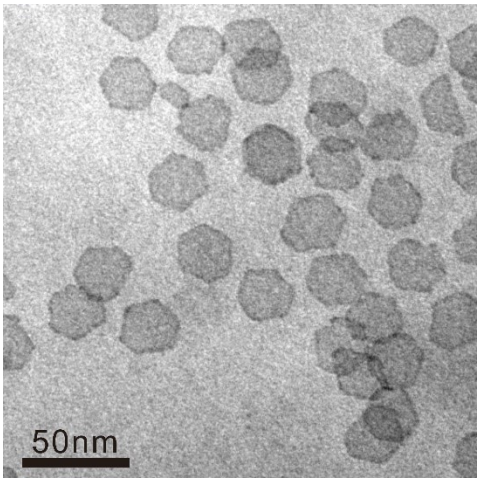

Figure S1. TEM image of 30 nm Pd.

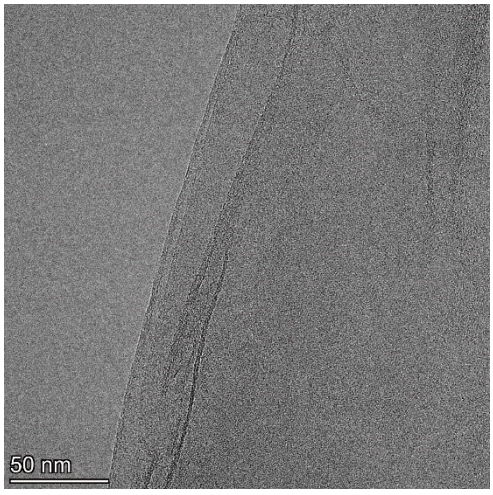

Figure S2. TEM image of GO.

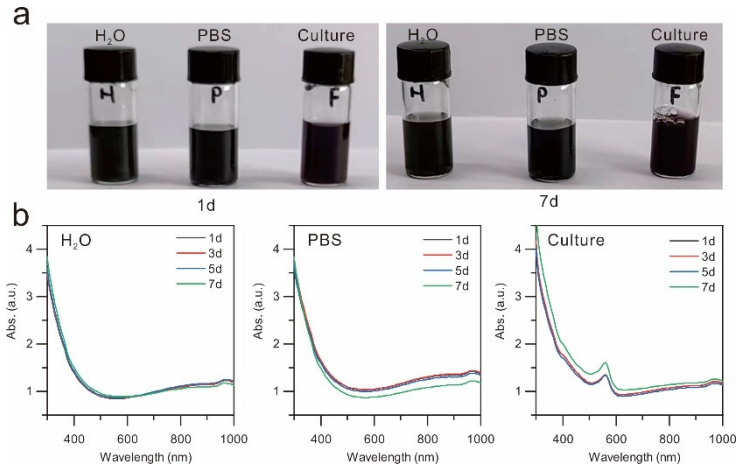

Figure S3. Dispersion stabilities of rGO-Pd in different solutions. (a) Photos of rGO-Pd dispersed in H_2O, PBS and culture medium within one week. (b) The corresponding absorption spectra of rGO-Pd in these media, respectively.

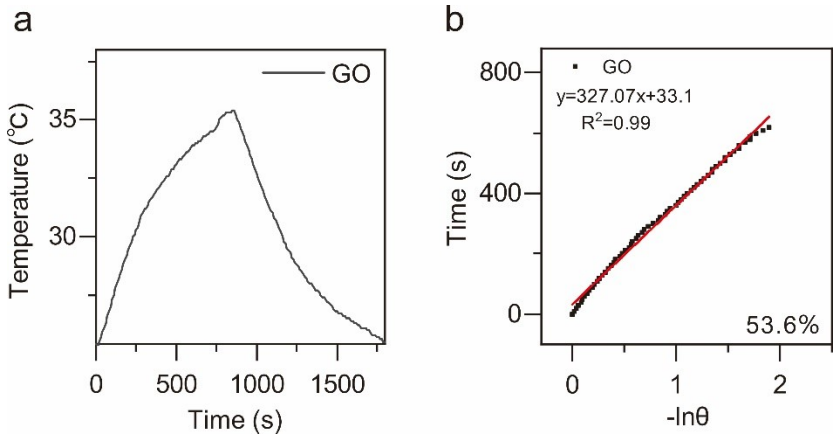

Figure S4. (a) The temporal temperature variation of 2 mL aqueous solution of GO (100 μg mL^{-1}). The solution is irradiated for 14 min using a 1 W cm^{-2} 808 nm laser, and cooled to room temperature under ambient environment. (b) The corresponding time constants for heat transfer by applying the linear time data from the cooling period versus negative natural logarithm of driving

force temperature.

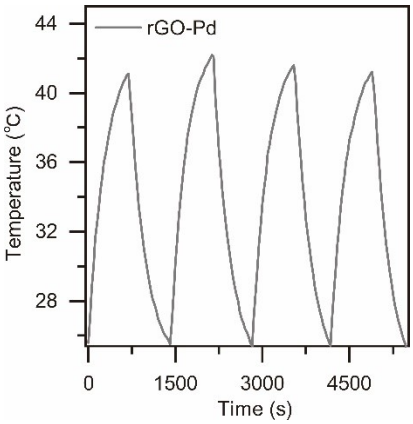

Figure S5. The photostabilities of rGO-Pd solutions after four cycles of 808 nm laser (1 W cm^{-2}) on/off.

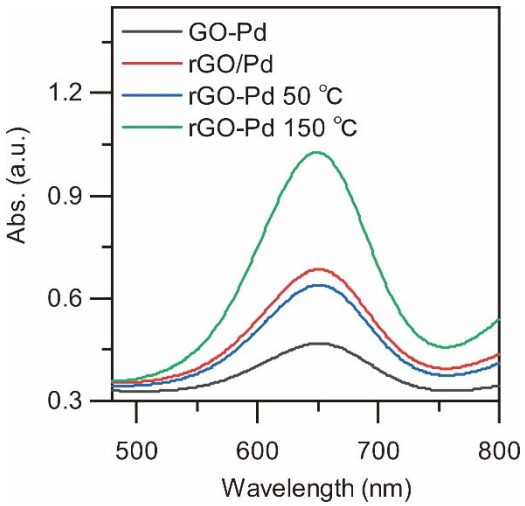

Figure S6. The absorbance changes at 652 nm of 0.5 mM TMB solutions containing 10 mM H_2O_2 with GO-Pd, rGO/Pd and rGO-Pd. Experiments were carried out in an acetic acid–sodium acetate buffer (pH 6)

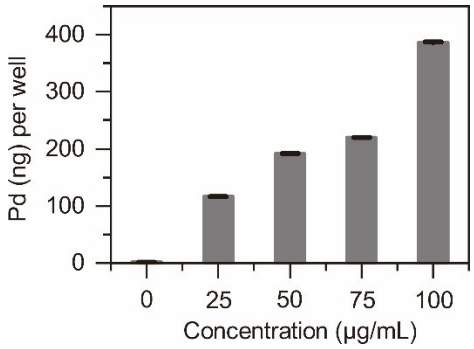

Figure S7. Quantitative cellular uptake of rGO-Pd by ICP-MS analysis.

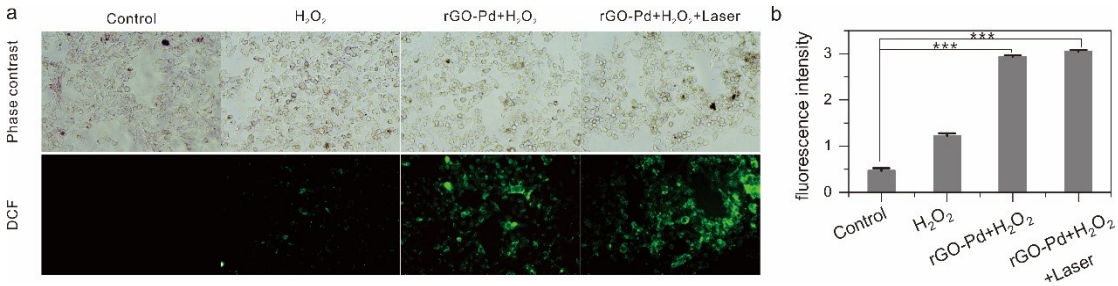

Figure S8. The intracellular ·OH generation of rGO-Pd (a) and quantitative ROS generation by microplate reader analysis. * indicates $p < 0.05$, ** indicates $p < 0.01$, *** indicates $p < 0.001$.

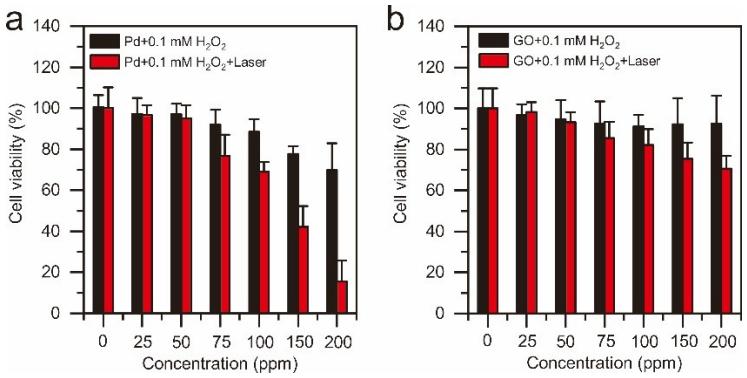

Figure S9. (a) The cytotoxicity of different concentrations of Pd with laser (0.5 W cm^{-2}) and without laser. (b). The cytotoxicity of different concentrations of GO with laser (0.5 W cm^{-2}) and without laser.

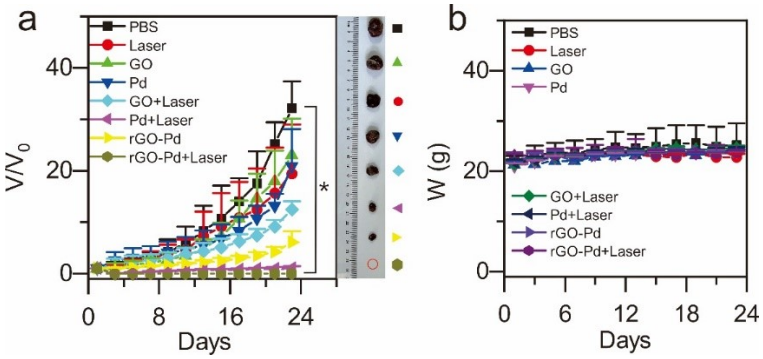

Figure S10. (a) Changes in tumor volumes of mice treated with different ways and photographs of the tumors in different groups at day 23 post administration. (b) Changes in weight of mice in different groups.

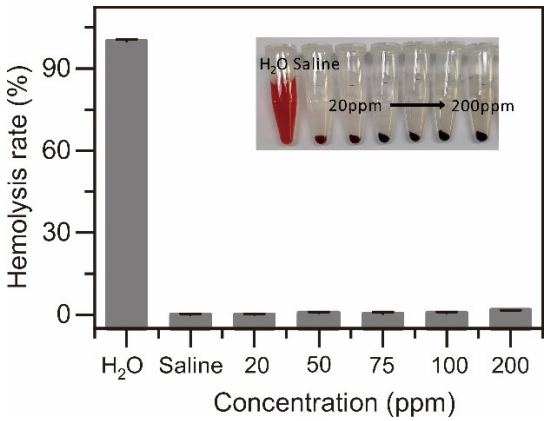

Figure S11. Quantitative results and photographs of hemolysis activity of rGO-Pd with different concentrations..

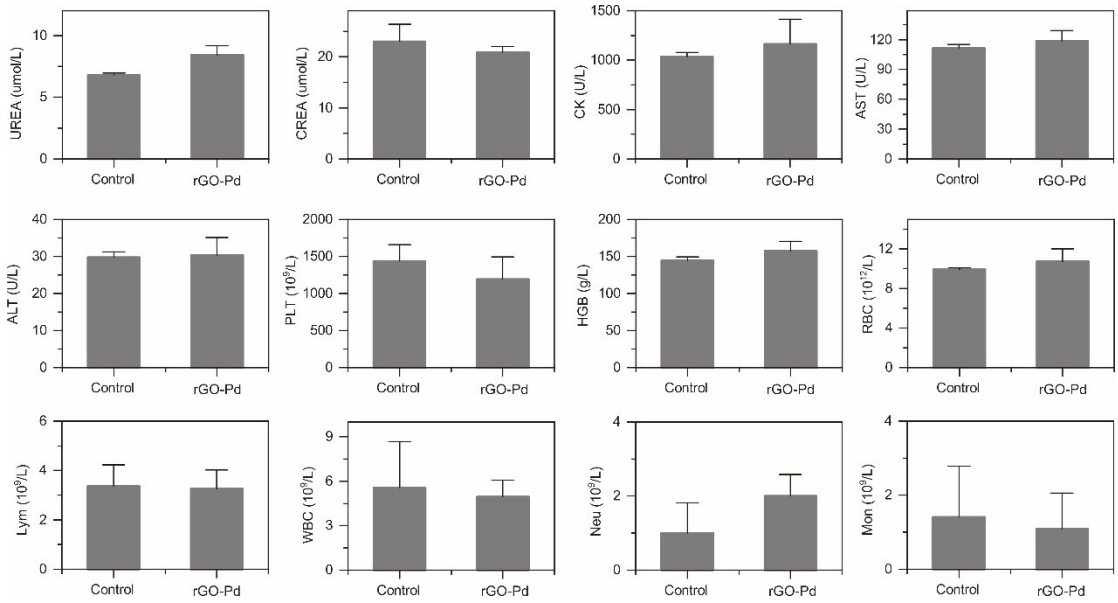

Figure S12. Some blood routine and biochemical indexes of mice after intravenous injection of rGO-Pd on day 14 after treatment..